

A New Narrow Resonance in the $D_s\pi^0$ System.

B. Meadows ¹

*University of Cincinnati*²
Cincinnati, OH, 45221, USA

Abstract. A sample of $\sim 91 \text{ fb}^{-1}$ of e^+e^- interactions at center of mass energy near $10.6 \text{ GeV}/c$ from the PEP-II asymmetric collider at SLAC has been examined by the *BABAR* collaboration. Evidence for a narrow state with mass $2317 \text{ MeV}/c^2$ decaying to $D_s^+\pi^0$ is found. These data, showing the signal and properties of the state, are presented. Evidence for a second state at $\sim 2460 \text{ MeV}/c^2$ decaying to $D_s s\pi^0$ is also shown. Data from other experiments are shown, and possible implications of the existence of these states discussed.

INTRODUCTION

Treating mesons made from one heavy and one light quark in a way analogous to the hydrogen atom [1] has met with considerable success in the understanding of D , D_s^+ , B and B_s mesons. If the mass m_h of the heavy quark is large, $m_h \gg \Lambda_s$, then the spin of the light quark (q) couples with the orbital angular momentum L to make a conserved quantity $j = L \pm 1/2$. This in turn combines with the spin of the charm quark to give total spin $J = j \pm 1/2$.

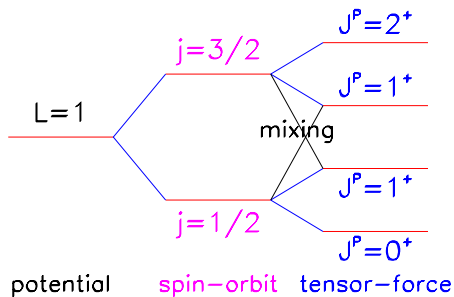


FIGURE 1. $L = 1$ states in the $c\bar{s}$ spectrum with the HQET coupling scheme. Forces involved include spin-orbit and tensor. Models differ somewhat in the way these are determined. If the condition $m_c \gg \Lambda_s$ is not fulfilled, then mixing between the two $J^P = 1^+$ states is possible.

This methodology has been used to compute masses and widths for charmed and charmed strange mesons [2, 3, 4, 5, 6]. The experimental situation for the positive parity ($L = 1$) states in the D_s spectrum, illustrated in fig. 1, is summarized in reference [7]. The two states with $j = 3/2$, expected to be narrow, are probably identified as the $J^P = 1^+$ $D_s(2536)$ seen in D^*K decay and (more speculatively) the $J^P = 2^+$ $D_{sJ}(2573)$ seen in

¹ Representing the Babar Collaboration

² Work supported by the National Science Foundation.

Work Supported in part by the Department of Energy Contract DE-AC03-76SF00515
Stanford Linear Accelerator Center, Stanford University, Stanford, CA 94309

Presented at the High-Energy Physics Workshop on Scalar Mesons:
An Interesting Puzzle for QCD Utica, New York, May 16-18, 2003

DK decays. Before the observations presented here became available, the two $j = 1/2$ states had yet to be observed. They were predicted to be well above thresholds for strong DK or D^*K decays respectively, at $\sim 2480 \text{ MeV}/c^2$ ($J^P = 0^+$) and $\sim 2560 \text{ MeV}/c^2$ ($J^P = 1^+$). Their large widths were expected to make them hard to observe.

The observations reported here (see *also reference* [8]) may provide evidence that these calculations are flawed and that these states may in fact be below strong decay threshold, and narrow.

THE *BABAR* DETECTOR

A full description of this solenoidal, magnetic spectrometer is given elsewhere [9]. A brief description follows. Charged particles are detected, and their momenta measured by a 40-layer drift chamber (DCH) barrel placed concentrically about a five-layer, double sided silicon vertex tracker (SVT) placed on the axis of the 1.5 T magnetic field provided by the superconducting solenoid. Charmed particle decay vertices are reconstructed with a typical resolution of $72 \mu\text{m}$ along the direction of the parent. Charged particle identification (PID) is accomplished with information from a Cherenkov ring imaging detector (DIRC) and with the measured energy loss (dE/dx) in the DCH and SVT. The DIRC radiator consists of 144 precisely polished, fused silica bars with rectangular cross section, arranged in a 12 sided configuration around the outer radius of the DCH. The bars transport, by total internal reflection, the Cherenkov photons they generate to a close packed array of photomultipliers placed at one end to allow reconstruction of the Cherenkov angle. Resolutions in this angle of $\sim 10 \text{ mrad}$ per photon (typically 2 mrad per track) are achieved, allowing clear distinction between charged K 's and π 's at the highest, kinematically possible momenta, $\sim 4.5 \text{ GeV}/c$. Detection of π^0 's and γ 's is accomplished with an electromagnetic calorimeter (EMC) made from CsI(Tl) crystals in a matrix with 56 (polar) by 120 (azimuthal) segmentation in a barrel and endcap configuration. Typical resolution in $\pi^0 \rightarrow \gamma\gamma$ mass is $2.5 \text{ MeV}/c^2$.

EVENT SELECTION

A sample of 91 fb^{-1} of available data, both on the $Y(4S)$ and below, are used. We seek to study events containing $D_s^+ \pi^0$ ³ combinations arising from a common vertex. Decays of D_s^+ to $K^+ K^- \pi^+$ and to $K^+ K^- \pi^+ \pi^0$ final states are chosen to provide a relatively clean sample. To avoid large combinatorial backgrounds from B decays, D_s^+ produced from $e^+ e^- \rightarrow c\bar{c}$ continuum interactions are selected by requiring the center of mass momentum $p^* > 2.5 \text{ GeV}/c$ - above the kinematic limit for B decay.

Events with at least three charged tracks and at least two clusters in the EMC are selected. A three track combination, of which two with opposite sign satisfy K^\pm PID requirements, are required to form a common vertex with chi squared probability greater

³ Throughout this paper, charge conjugate states are implied unless explicitly stated otherwise.

than 0.1%.

Photon pairs that can be constrained to point to either the primary or the $K^+K^-\pi^+$ vertex, and to have a π^0 mass are used to define π^0 candidates. Pairs which include a γ shared by another π^0 are excluded from further consideration.

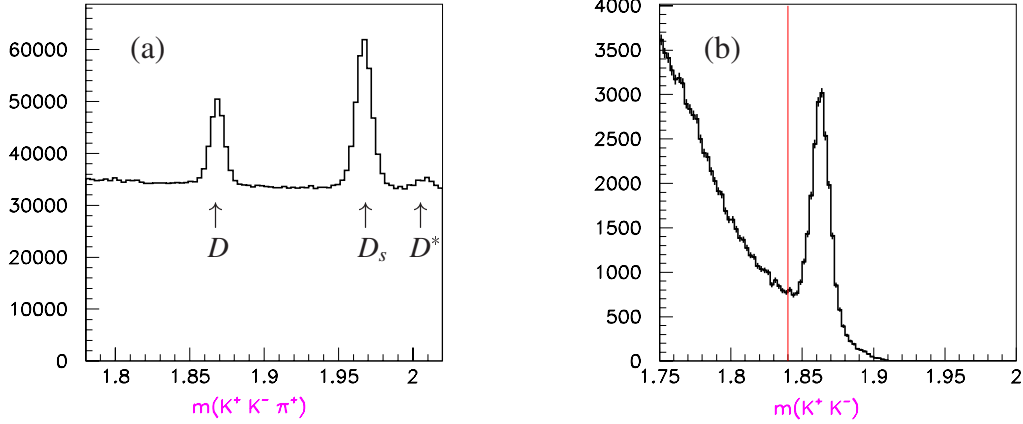


FIGURE 2. (a) Effective mass of $K^+K^-\pi^+$ combinations before ϕ or \bar{K}^{*0} cuts. Signals at D^+ , D_s^+ masses are clearly seen. A small D^{*+} is also seen. (b) Effective mass of K^+K^- system showing the D^0 from the D^{*+} decay in (a). Removing events with $m_{KK} > 1840$ MeV/ c^2 eliminates this source of background.

The $D_s^+ \rightarrow K^+K^-\pi^+$ invariant mass distribution in fig. 2a of these combinations shows D_s^+ and D^+ signals. A small but significant signal is also seen at the D^{*+} which decays to $D^0\pi^+$ with subsequent decay $D^0 \rightarrow K^+K^-$. This is easily removed as a potential source of background to the D_s^+ by removing K^+K^- combinations with mass, shown in fig. 2 b, above 1840 MeV/ c^2 . Background is greatly reduced when $\phi\pi^+$ and $\bar{K}^{*0}K^+$ modes are selected by requiring that $|M_{K^+K^-} - 1019| < 10$ MeV/ c^2 and $|M_{\pi^+K^-} - 896| < 50$ MeV/ c^2 respectively. In each of these modes, selection of events with $|\cos\vartheta_v| > 0.5$, where ϑ_v is the angle between the pseudo scalar bachelor particle and the K^- in the vector (ϕ or \bar{K}^{*0}) rest frame, further improves the signal to background ratio for the D_s^+ . This is shown in fig. 3a. Signal and sideband regions are defined in this figure by the shaded areas. Approximately 80,000 $D_s^+ \rightarrow \phi\pi^+$ or $\rightarrow \bar{K}^{*0}K^+$ events remain.

To define a sample of $D_s^+ \rightarrow K^+K^-\pi^+\pi^0$ decays, candidates for $K^+K^-\pi^+$ combinations are combined with π^0 's refitted as before but constrained to point back to the $K^+K^-\pi^+$ vertex. Clear signals for both D^+ and for D_s^+ to decay in this 4-body mode are seen, though backgrounds are larger than for the 3-body decays. Background is reduced by requiring π^0 's to have momentum > 300 MeV/ c . The 2-body subsystems in these D_s^+ decays are found to be strongly resonant. Selection of two body sub systems in the $\bar{K}^0, K^{*+}, \rho^+$ or ϕ mass ranges improves the signal more. Signal and background regions were defined for D_s^+ decaying in this mode as before.

THE SIGNAL

Fig. 3b shows the effective mass distribution of $D_s^+ \pi^0$ combinations. A striking, narrow signal is seen at a mass of 2317 MeV/c^2 . Also seen is the D_s^{*+} decaying to $D_s^+ \pi^0$, a well established, isospin violating mode observed first in the CLEO experiment [10]. Neither signal is seen however in the D_s^+ sidebands (shaded distribution in fig. 3b). Fig. 4a shows

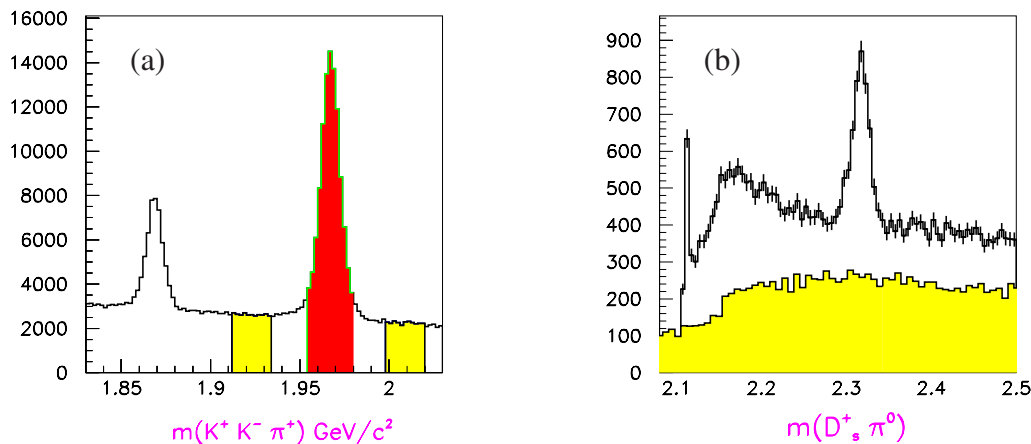


FIGURE 3. (a) Effective mass of $\phi\pi^+$ and $\bar{K}^0 K^+$ combinations after applying cuts described in the text. D_s^+ signal ($1954 < m_{KK\pi} < 1980$) and sideband ($1912 < m_{KK\pi} < 1934$ and $1912 < m_{KK\pi} < 193$) regions are indicated by dark and light shading, respectively. (b) Distributions of $K^+ K^- \pi^+ \pi^0$ effective masses. The unshaded distribution is for events in the D_s^+ signal region and the shaded one is for events in the D_s^+ sidebands.

the effective mass distribution of pairs of photons with energies above 100 MeV, and indicates a clear presence of π^0 's in the sample. Signal and sideband regions are defined as indicated. The signal at 2317 MeV/c^2 is seen in fig. 4b where $K^+ K^- \pi^+ \gamma\gamma$ effective mass combinations are plotted when $K^+ K^- \pi^+$ and $\gamma\gamma$ masses are in the D_s^+ and π^0 signal regions respectively (unshaded plot). The D_s^{*+} is smeared however since the $\gamma\gamma$ mass is not constrained to the π^0 mass. The signal at 2317 MeV/c^2 is not seen in the π^0 sidebands (shaded events).

A New State

Before claiming this peak as a new state, it is important to check that it behaves appropriately.

We first check that the signal is not a reflection produced by any known state. We study a sample of approximately 80×10^6 interactions of the type $e^+ e^- \rightarrow c\bar{c}$, simulated to include all that is presently known about charm spectroscopy. These events are subjected to the effects of the BABAR spectrometer and then processed through the same reconstruction and selection programs as were the data. The $K^+ K^- \pi^+$ and $D_s^+ \pi^0$ mass distributions are shown in fig. 5. Signals for D^+ and D_s^+ are clear, as is that for

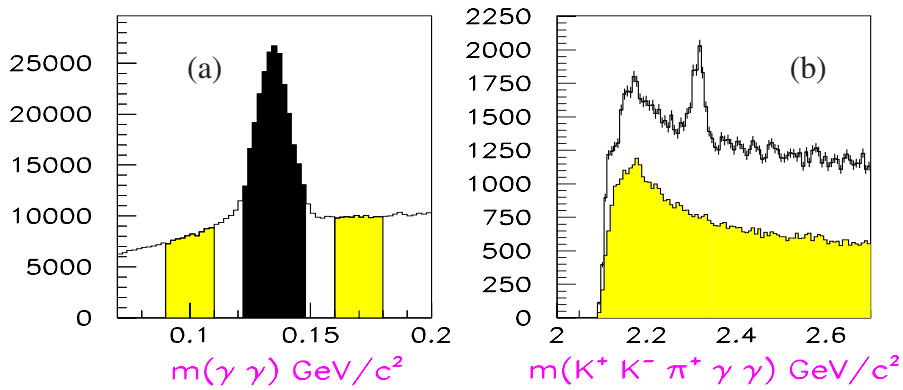


FIGURE 4. (a) Effective mass of $\gamma\gamma$ combinations. Energy of each γ , $E_\gamma > 100$ MeV. Signal and sideband regions are indicated by dark and light shading, respectively. (b) Distributions of $K^+K^-\pi^+\gamma\gamma$ effective masses for events in the D_s^+ signal region defined in fig. 2b. The unshaded distribution is for events in the π^0 signal region and the shaded one is for events in the π^0 sidebands.

$D_s^{*+} \rightarrow D_s^+\pi^0$, but there is clearly no evidence for the signal at $2317 \text{ MeV}/c^2$. We conclude that the signal at $2317 \text{ MeV}/c^2$ in the data does not arise from reflection of any known state.

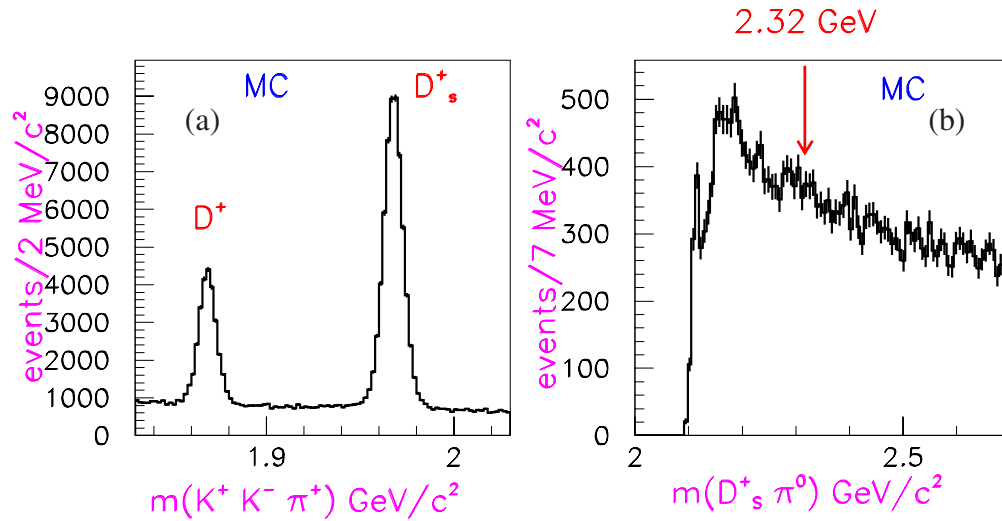


FIGURE 5. (a) Effective mass of $\phi\pi^+$ and $\bar{K}^{*0}K^+$ combinations after applying cuts described in the text to a simulated sample of $\sim 80 \times 10^6 e^+e^- \rightarrow c\bar{c}$ interactions. D^+ and D_s^+ signals are clearly seen. (b) Distributions of $D_s^+\pi^0$ effective mass combinations from the same simulated events. A signal for $D_s^{*+} \rightarrow D_s^+\pi^0$ decays is evident, but there is no $D_{sJ}(2317)^+$ signal.

We next check that the signal appears in data from both $D_s^+ \rightarrow \phi\pi^+$ and $D_s^+ \rightarrow \bar{K}^{*0}K^+$ decay modes. These are shown in figs. 6a and b, respectively. The signal is evident in both modes.

We also look at events in our $D_s^+ \rightarrow K^+ K^- \pi^+ \pi^0$ sample. Fig. 6c shows the effective mass distribution obtained when these systems are combined with a further π^0 . Events in the D_s^+ signal region (unshaded) show the peak at 2317 MeV/c^2 while events in the sidebands (shaded) do not. The 2317 signal appears to be produced in the same ratio

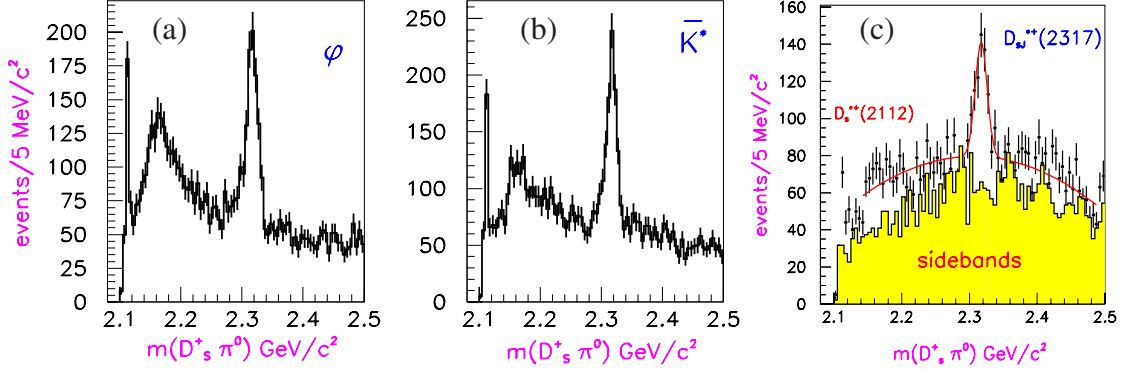


FIGURE 6. Effective mass of $D_s^+ \pi^0$ combinations for (a) $D_s^+ \rightarrow \phi \pi^+$ events, (b) $D_s^+ \rightarrow \bar{K}^{*0} K^+$ events, (c) $D_s^+ \rightarrow K^+ K^- \pi^+ \pi^0$ events,

with respect to the $D_s^{*+} \rightarrow D_s^+ \pi^0$ signal in $\phi \pi$ and $\bar{K}^{*0} K^+$ modes. This ratio is not the same, however as that observed in fig. 6c for the the $K^+ K^- \pi^+ \pi^0$ mode. This is explained by observing that, in the 4 body decay mode, events are subjected to a greater photon energy cut, thus altering the D_s^+ momentum spectrum.

We conclude that the signal at 2317 MeV/c^2 is most likely a new, narrow resonance that decays to $D_s^+ \pi^0$, and we label it $D_{sJ}(2317)^+$.

PROPERTIES OF $D_{sJ}(2317)^+$

Momentum Spectrum

Using the events in the $\phi \pi^+$ and $\bar{K}^{*0} K^+$ modes, we examine the production rate (for the $D_s^+ \pi^0$ decay mode of this state) as a function of p^* . In fig. 7 distributions of $D_s^+ \pi^0$ effective mass are shown for events in discrete ranges of p^* .

The signal is clearly seen in each range, and the background becomes less significant as p^* increases. This behaviour is expected of a charm particle produced in $e^+ e^-$ interactions at the $Y(4S)$ energy as B decays become less important as p^* increases. These distributions are fitted with a Gaussian function on a second order polynomial background and a number of signal events determined for each range. A simulated sample of $D_{sJ}(2317)^+$ decays is used to determine the efficiency, and the corrected production rates computed in each p^* range. The results are shown in fig. 8. The data appear to demonstrate a production rate that peaks in the 3-4 GeV/c range. For further studies, we require that $p^* > 3.5 \text{ GeV}/c$.

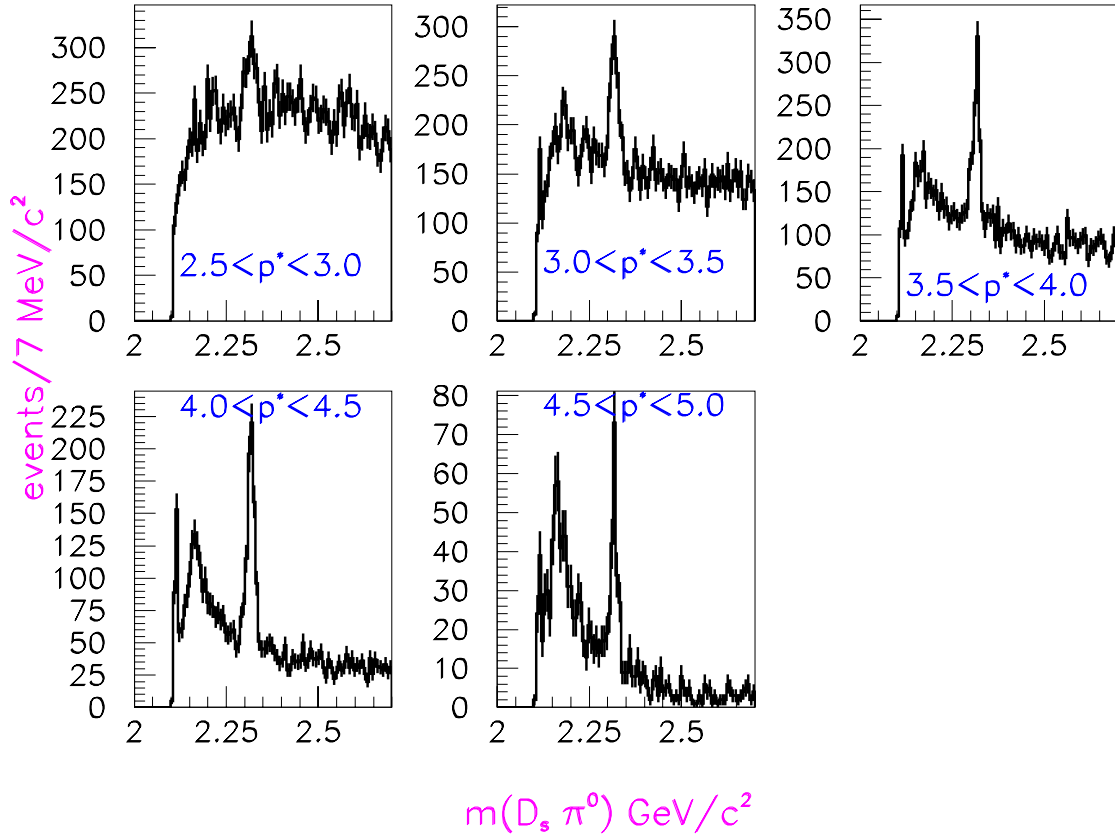


FIGURE 7. $D_s^+\pi^0$ invariant mass distributions in five, discrete center of mass momentum (p^*) ranges.

Decay Angular Distribution

The distribution of the angle ϑ between the π^0 and the $D_{sJ}(2317)^+$, boosted to the $D_{sJ}(2317)^+$ rest frame, can reveal information about the spin-parity of the state. The $D_s^+\pi^0$ sample is divided into 10 ranges of $\cos\vartheta$ and signal yields determined for each with fits similar to those used for the p^* study. The simulated sample of $D_{sJ}(2317)^+ \rightarrow D_s^+\pi^0$ decays was used to determine the efficiency in each range, and the acceptance corrected angular distribution was determined. These results are presented in fig. 9.

The distribution can be described as having no $\cos\vartheta$ dependence. This is consistent with $J^P = 0^-$, but this is not conclusive evidence for this assignment. For higher spins, a flat distribution would also be expected for a completely unaligned production. Our data are produced in continuum interactions, and there is no prediction for the $D_{sJ}(2317)^+$ alignment. Were the $D_{sJ}(2317)^+$'s produced in B decay with a recoil D^4 for example, they would be aligned with helicity zero. In that case, higher spins would produce

⁴ We note that since this talk was given, the BELLE collaboration has observed a flat distribution in $B \rightarrow DD_{sJ}(2317)^+$ decays, indicating $J^P = 0^-$.

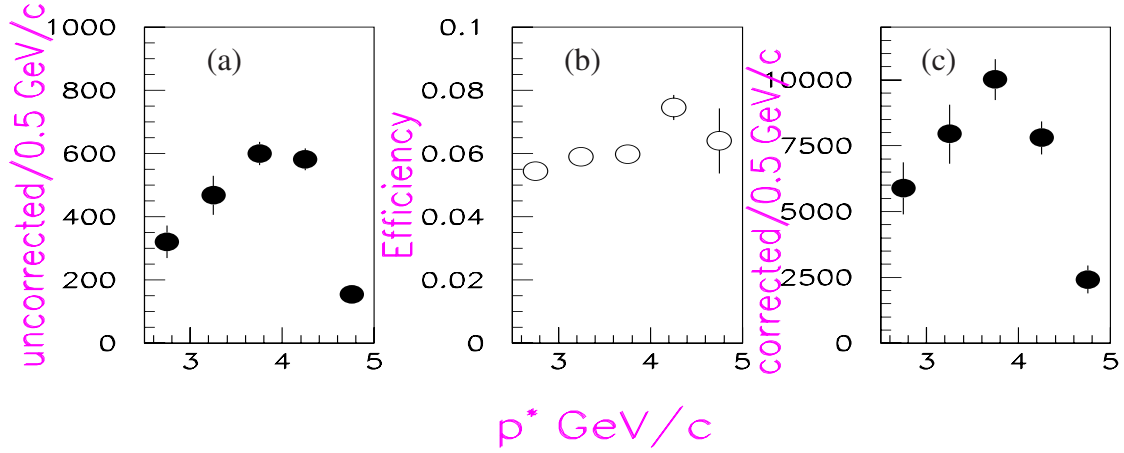


FIGURE 8. Dependence on p^* of (a) signal yields, derived from fits described in the text to the invariant mass distributions in fig. 7; (b) reconstruction efficiencies; (c) corrected yields.

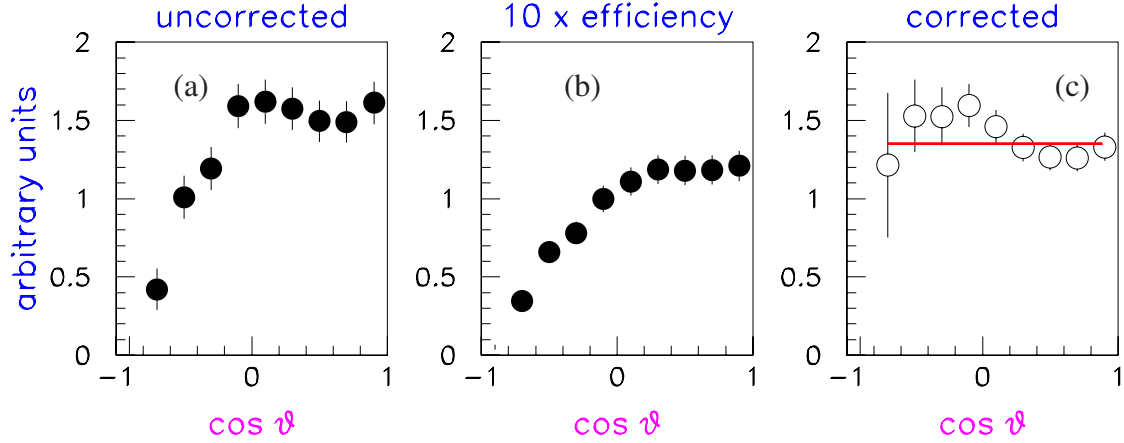


FIGURE 9. (a) Signal yield (arbitrary units) derived from fits described in the text to the invariant mass distributions in 10 ranges of $\cos \vartheta$. (b) Reconstruction efficiencies determined from a sample of simulated $D_{sJ}(2317)^+ \rightarrow D_s^+ \pi^0$ decays (produced with no natural width) in the same ranges. (c) Corrected signal yields.

distributions that would not be flat at all.

We conclude that with the present data sample, we are unable, on the basis of the observed decay distribution, to rule out spins greater than $J = 0$.

Mass and Width

We fit $D_s^+ \pi^0$ invariant mass distributions for both $D_s^+ \rightarrow K^+ K^- \pi^+$ and $D_s^+ \rightarrow K^+ K^- \pi^+ \pi^0$ shown in figs. 10a and b respectively, requiring that $p^* > 3.5$ GeV/c. We use Gaussian functions to describe signals and third order polynomials for the backgrounds. Masses from each sample are in excellent agreement. For the $K^+ K^- \pi^+$ sample,

the signal contains 1267 ± 53 events with $m = 2316.8 \pm 0.4 \text{ MeV}/c^2$ and for $K^+K^-\pi^+\pi^0$ the fit gives 273 ± 33 events with $m = 1217.6 \pm 1.3 \text{ MeV}/c^2$. We quote statistical errors only; however, we believe that mass scale uncertainties are less than $1 \text{ MeV}/c^2$.

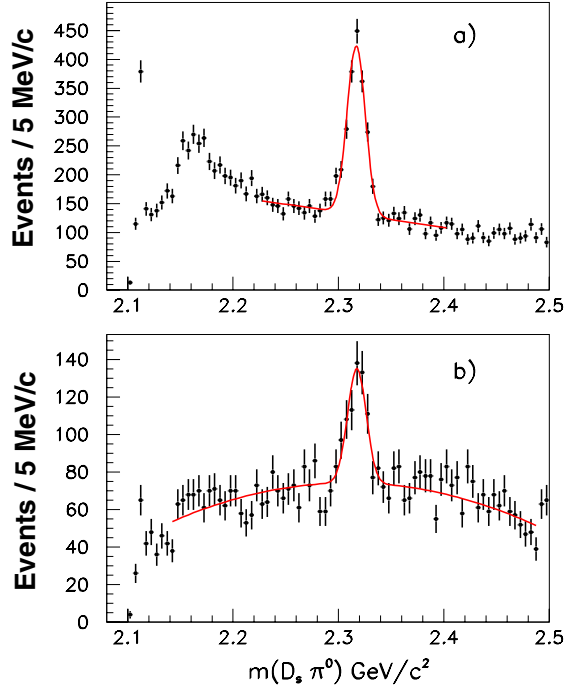


FIGURE 10. Invariant mass distributions for $D_s^+ \pi^0$. Fits shown are to a Gaussian function describing the $D_{sJ}(2317)^+$ signal and a third order polynomial for the background. Results of the fits are given in the text. Plots are for (a) $D_s^+ \rightarrow \phi \pi^+$ and $D_s^+ \rightarrow \bar{K}^{*0} K^+$; (b) $D_s^+ \rightarrow K^+ K^- \pi^+ \pi^0$ events.

The widths determined in the two fits also agree well - 8.6 ± 0.4 and $8.8 \pm 1.1 \text{ MeV}/c^2$ respectively. The resolution for the first system was estimated from events simulating the decays $D_{sJ}(2317)^+ \rightarrow D_s^+ \pi^0$, and $D_s^+ \rightarrow \phi \pi^+ (\bar{K}^{*0} K^+)$, where the $D_{sJ}(2317)^+$ was assigned a width of just $1 \text{ MeV}/c^2$. The result found was $9.0 \pm 0.4 \text{ MeV}/c^2$. Since the D_s^+ mass is constrained to the PDG [11] value, the resolution of both modes is virtually the same. The measured widths, therefore, are compatible with the resolution. We can safely say that the natural width if the $D_{sJ}(2317)^+$ is less than $10 \text{ MeV}/c^2$, though there is no reason why it cannot be much narrower than that.

SEARCH FOR OTHER DECAY MODES OF $D_{sJ}(2317)^+$

Other decay modes investigated include:

$$\begin{aligned}
 D_{sJ}(2317)^+ &\rightarrow D_s^+ \gamma \\
 &\rightarrow D_s^+ \gamma \gamma \\
 &\rightarrow D_s^{*+} \gamma \\
 &\rightarrow D_s^+ \pi^0 \pi^0
 \end{aligned}$$

$$\rightarrow D_s^+ \pi^0 \gamma$$

In all cases, to reduce combinatorial backgrounds, we require that γ 's be unassociated

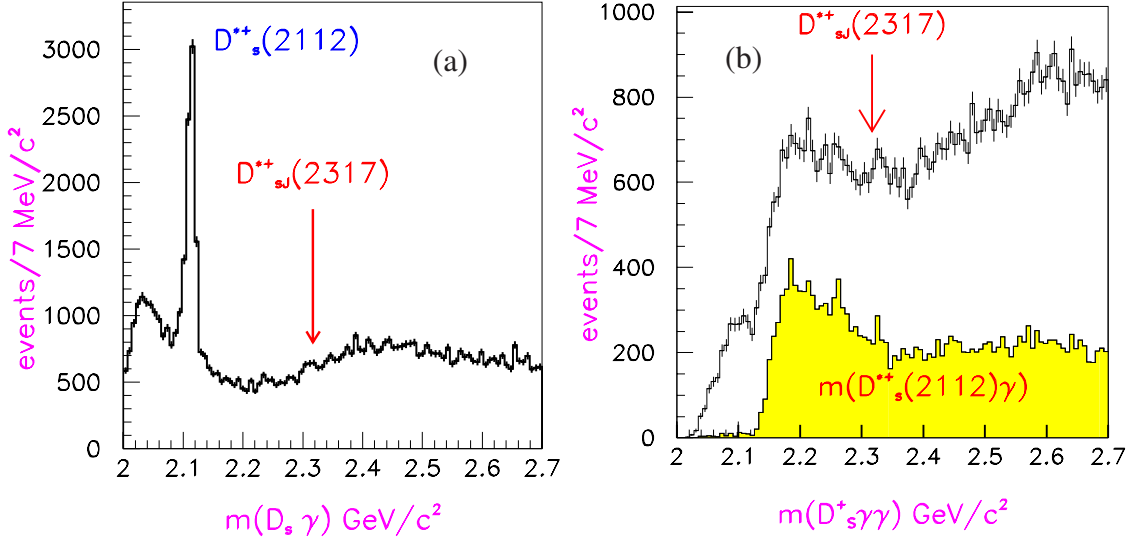


FIGURE 11. Distribution of invariant mass combinations of $D_s^+ \rightarrow \phi \pi^+$ and $D_s^+ \rightarrow \bar{K}^{*0} K^+$ with γ 's. Events have $p^* > 3.5$ GeV/c and no γ forms part of any π^0 candidate. (a) $D_s^+ \gamma$ combinations; (b) $D_s^+ \gamma\gamma$ combinations (unshaded histogram) and $D_s^{*+} \gamma$ combinations (shaded histogram).

with any π^0 . Also, photons with E_γ were not considered. Only events from the $D_s^+ \rightarrow \phi \pi^+$ and $D_s^+ \rightarrow \bar{K}^{*0} K^+$ samples were studied. To avoid bias, events having no π^0 at all were included in the analysis.

Fig. 11a and b show the $D_s^+ \gamma$ and $D_s^+ \gamma\gamma$ mass combinations, respectively. The D_s^{*+} signal is seen to dominate the $D_s^+ \gamma$ plot. No other signal, particularly at 2317, is evident in either plot. The shaded region in fig. 11b is the distribution of $D_s^{*+} \gamma$ effective masses. Again, no signal is seen.

Fig. 12a shows the $D_s^+ \pi^0 \pi^0$ mass combinations. No signal is seen at 2317 MeV/c². Fig. 12b is the $D_s^+ \pi^0 \gamma$ mass distribution. Again, no signal is seen at 2317 MeV/c². Structure is evident at about 2460 MeV/c² however. This becomes very prominent when events that have $D_s^+ \gamma$ invariant mass in the D_s^{*+} signal region.

Another State?

This $D_s^+ \pi^0 \gamma$ signal at 2460 MeV/c² occurs where the $D_s^+ \gamma$ effective mass is largely in the D_s^{*+} signal region. Kinematically, events in this region also have their $D_s^+ \pi^0$ effective mass largely in the $D_{sJ}(2317)^+$ signal region. We estimate that at most one sixth of the $D_{sJ}(2317)^+$ signal coincides with this signal. Also, the projection of the signal onto the $D_s^+ \pi^0$ mass axis is approximately 12 MeV/c² wide. For these reasons, we discount the possibility that the $D_{sJ}(2317)^+$ is a reflection of this new state at 2460 MeV/c². On the other hand, the $D_{sJ}(2317)^+$ provides a peaking background under the 2460 signal (see fig. 13c), and appears to account for a large part of it.

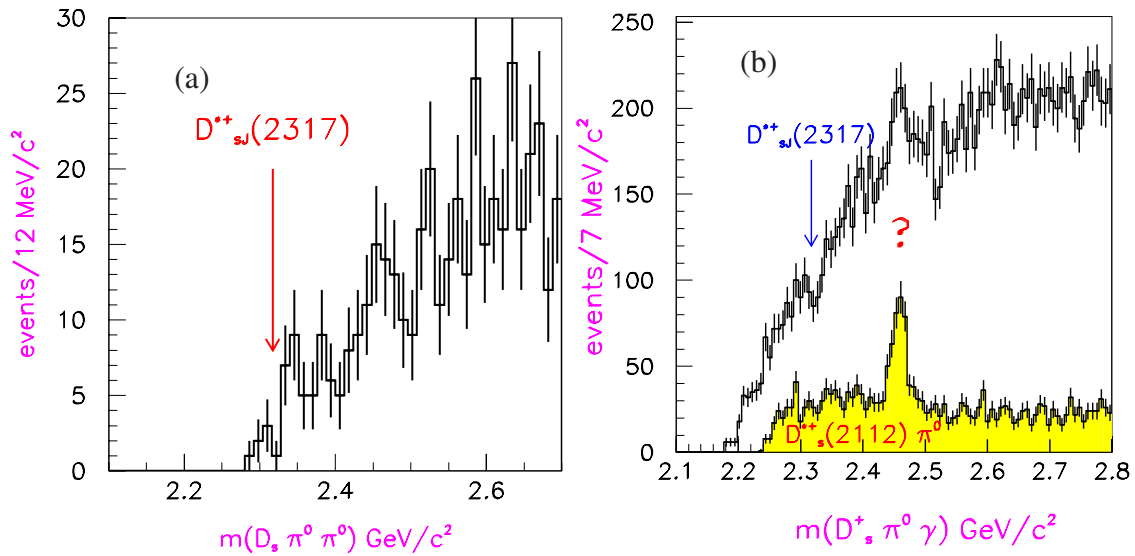


FIGURE 12. Distribution of invariant mass combinations for $D_s^{*+} \rightarrow \phi \pi^+$ and $D_s^{*+} \rightarrow \bar{K}^{*0} K^+$ samples. Events have $p^* > 3.5$ GeV/c and no γ forms part of any π^0 candidate. (a) $D_s^{*+} \pi^0 \pi^0$ combinations; (b) $D_s^{*+} \pi^0 \gamma$ combinations (unshaded histogram) and $D_s^{*+} \pi^0$ combinations (shaded histogram).

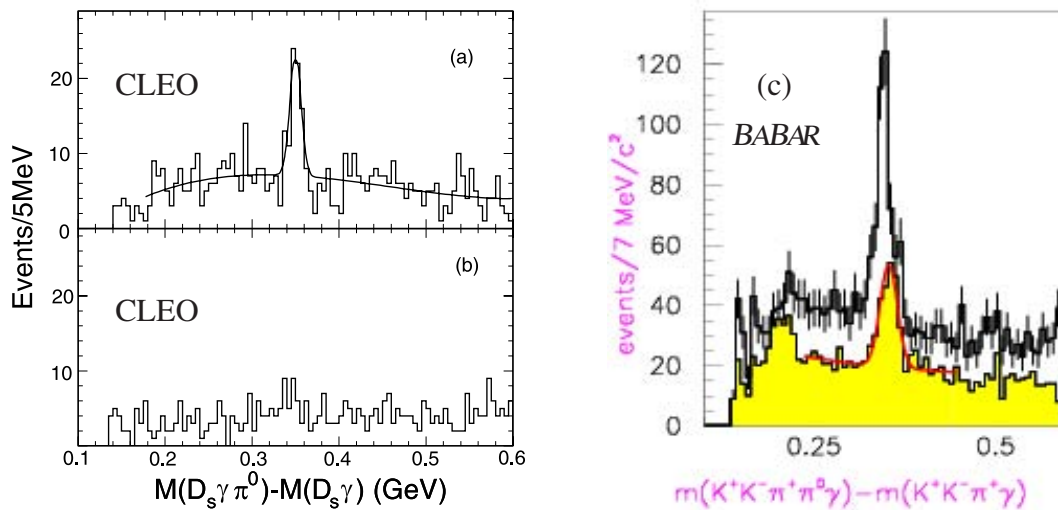


FIGURE 13. Invariant mass difference $\Delta m = m(K^+ K^- \pi^+ \pi^0 \gamma) - m(K^+ K^- \pi^+ \gamma)$ for: (a) CLEO, 13.5 fb^{-1} data. Events are in the D_s^{*+} signal region. (b) The same as in (a) for events in the D_s^{*+} sidebands. (c) *BABAR* 91 fb^{-1} data. Unshaded histogram is for events in the D_s^{*+} signal region. The shaded histogram is for events in the D_s^{*+} sidebands. The peaking of the sideband background is more pronounced in the *BABAR* data than in CLEO's.

The CLEO collaboration now reports observing this signal, claiming it as a new state. Their yield (per fb^{-1}) corresponds to about three times that observed by *BABAR*. Fig. 13a shows their signal and fig. 13b shows the corresponding $D_{sJ}(2317)^+$ sideband distribution. The latter shows some peaking, though it appears to be somewhat less pronounced and to account for less of the 2460 signal.

To make a quantitative estimate of the fraction of this signal that is due to a new state, and how much is due to $D_{sJ}(2317)^+$ reflection, a multi dimensional fit to all effective masses is most likely to provide the right answer. Such an analysis forms part of the ongoing effort in the *BABAR* collaboration.

CORROBORATION BY OTHER EXPERIMENTS

The CLEO collaboration, using a sample of 13.5 fb^{-1} , with $D_s^+ \rightarrow \phi \pi^+$, confirms [12] seeing clear evidence for $D_{sJ}(2317)^+$ in the $D_s^+ \pi^0$ decay mode (see fig. 14)

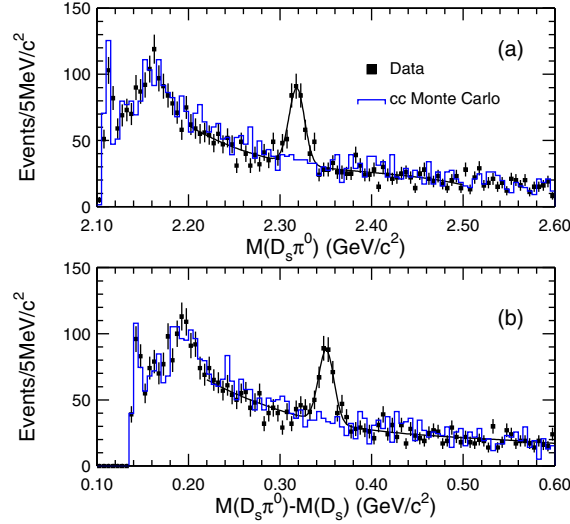


FIGURE 14. Distribution of invariant mass combinations of $D_s^+ \pi^0$ from the CLEO collaboration in reference [12]. (a) $D_s^+ \pi^0$ mass; (b) $m(K^+ K^- \pi^+ \pi^0) - m(K^+ K^- \pi^+)$. The $D_{sJ}(2317)^+$ peak is evident. The curve under the peak in each case is the distribution of generic $c\bar{c}$ events.

Their signal has 231_{-29}^{+31} events. This corresponds to a yield per fb^{-1} almost equal to *BABAR*'s. They also search for decays to $D_s^+ \gamma$, $D_s^{*+} \gamma$ or $D_s^+ \pi^+ \pi^-$ with no signal found.

Since this talk was given, the BELLE collaboration has also reported the $D_{sJ}(2317)^+$ signal in both $B \rightarrow DD_{sJ}(2317)^+$ [13] and in $c\bar{c}$ continuum [14] production modes. They also report seeing the $D_{sJ}(2460)^+$ in both production modes and with decays to $D_s^{*+} \pi^0$ and to $D_s^+ \gamma$. *BABAR* also sees these signals.

DISCUSSION AND SUMMARY

The $D_{sJ}(2317)^+$ is too light to decay strongly to DK . The decay $D_{sJ}(2317)^+ \rightarrow D_s^+ \pi^0$ does not conserve isospin. This provides a good explanation for this state to be narrow. Decay to $D_s^+ \pi^0$ requires a natural spin-parity. Absence of decay to $D_s^+ \gamma$ suggests that $J^P \neq 1^-$. This makes a 0^+ assignment most likely, and this is consistent with absence of a $D_s^+ \pi^0 \pi^0$ (or $D_s^+ \pi^+ \pi^-$) decay. Though OZI suppressed, these modes conserve isospin, and are consistent with strong decay for all natural spin-parities except for $J^P = 0^+$. Similarly, the state at $\sim 2460 \text{ MeV}/c^2$, between DK and $D^* K^0$ thresholds, also fails

to decay strongly, suggesting unnatural parity. The possibility of identifying it as the missing $J^P = 1^+$ state in the $L = 1$ spectrum is hard to ignore.

The electromagnetic decay $D_{sJ}(2317)^+ \rightarrow D_s^{*+} \gamma$ (p wave) could compete with $D_s^+ \pi^0$ (s wave). The latter mode probably involves strong decay to $D_s^+ \eta$ (*virtual*) followed by $\eta - \pi^0$ mixing, as suggested by Cho and Wise [15]. Future measurement of the ratio of these modes could provide useful information relevant to this mechanism.

The mass of the $D_{sJ}(2317)^+$, 42 MeV/ c^2 below DK threshold, results in a small width, thus making it easier to observe. However this mass is approximately 170 MeV/ c^2 below that expected in the earlier predictions which for other states were typically within ~ 10 MeV/ c^2 of those observed.

An attempt to tune the relative strength of spin-orbit and tensor forces involved in the hydrogen atom-like computation of D and D_s states with $L = 1$ has been made by Cahn and Jackson [16] They took the $D_{sJ}(2317)^+$ mass as input (in addition to that of the two $j = 3/2$ states) and were able to predict the remaining $J^P = 1^+$ $c\bar{s}$ state at either 2406 or 2480 MeV/ c^2 . This approach introduced two new parameters.

The low mass of the $D_{sJ}(2317)^+$ has also prompted discussion on the possibility that it may be related to the light scalar states just below $K\bar{K}$ threshold, $f_0(980)$ ($I=0$) or $a_0(980)$ ($I=1$), whose makeup is generally believed to be other than that of simple $q\bar{q}$ pairs. Thus the $D_{sJ}(2317)^+$ (and probably the 2460 state too) would be perceived as either a four quark state, or even a DK molecule [17] with a 42 MeV binding energy. This would lead to the expectation that other charge modes could be seen in $D_s^+ \pi^+$ and $D_s^+ \pi^-$. The CDF II collaboration has attempted to find these, so far in vain ⁵.

Rupp and Van Beveran [18] interpret $D_{sJ}(2317)^+$ as an expected feature of DK scattering, quite analogous to $\pi\pi$ or to $K\pi$ scattering, and independent of any model for its composition. Bardeen, Eichten and Hill [19], predict an equal mass spacing between chiral partners $D_s^+ (0^-) / D_{sJ}(2317)^+ (0^+)$ and $D_s^{*+} (1^-) / D_s^+ (1^+)$ which would place the latter state at a mass of just about 2460 MeV/ c^2 .

Much other theoretical discussion has begun [20, 21, 22, 23]. No doubt more will follow. Possibly models with mixed states of $c\bar{s}$, 4 quark and molecule will be considered. A revival of discussion of penta quark states, $\bar{K}N$ bound states such as $\Lambda_s(1405)$ or its charm analogue also seems likely.

In summary, a new state with mass 2317 MeV/ c^2 decaying to $D_s^+ \pi^0$ is established to exist. Its width is comparable to the resolution in this system, so the natural width may be very small, but is certainly less than 10 MeV/ c^2 . No evidence for decay to $D_s^+ \gamma$, $D_s^{*+} \gamma$, $D_s^+ \gamma\gamma$, $D_s^+ \pi^0 \gamma$ or $D_s^+ \pi^0 \pi^0$ is seen. The CLEO collaboration confirm the existence of this state, with no evidence for decays to $D_s^+ \gamma$, $D_s^{*+} \gamma$ or $D_s^+ \pi^+ \pi^-$. The BELLE experiment further confirms these results. A second state at ~ 2460 MeV/ c^2 , with width comparable to resolution, has also been established ⁶ to exist.

⁵ Private communication, Christoph Paus, SLAC Seminar, June 2003.

⁶ Since the time this talk was given, this has also been observed by all three experiments and seen to decay to both $D_s^{*+} \pi^0$ and to $D_s^+ \gamma$. Both states have also been seen in B decays with recoil D meson. Angular distributions [13] indicate $J^P = 0^+$ for $D_{sJ}(2317)^+$ and $J^P = 1^+$ for $D_{sJ}(2460)^+$.

ACKNOWLEDGEMENTS

We are grateful for the extraordinary contributions of our PEP-II colleagues in achieving the excellent luminosity and machine conditions that have made this work possible. The success of this project also relies critically on the expertise and dedication of the computing organizations that support *BABAR*. The collaborating institutions wish to thank SLAC for its support and the kind hospitality extended to them. This work is supported by the US Department of Energy and National Science Foundation, the Natural Sciences and Engineering Research Council (Canada), Institute of High Energy Physics (China), the Commissariat à l’Energie Atomique and Institut National de Physique Nucléaire et de Physique des Particules (France), the Bundesministerium für Bildung und Forschung and Deutsche Forschungsgemeinschaft (Germany), the Istituto Nazionale di Fisica Nucleare (Italy), the Foundation for Fundamental Research on Matter (The Netherlands), the Research Council of Norway, the Ministry of Science and Technology of the Russian Federation, and the Particle Physics and Astronomy Research Council (United Kingdom). Individuals have received support from the A. P. Sloan Foundation, the Research Corporation, and the Alexander von Humboldt Foundation.

REFERENCES

1. De Rujula, A., Georgi, H., and Glashow, S. L., *Phys. Rev. Lett.*, **37**, 785-788 (1976).
2. Godfrey, S., and Isgur, N., *Phys. Rev.*, **D32**, 189–231 (1985).
3. Isgur, N., and Wise, M. B., *Phys. Rev. Lett.*, **66**, 1130–1133 (1991).
4. Godfrey, S., and Kokoski, R., *Phys. Rev.*, **D43**, 1679–1687 (1991).
5. Bardeen, W. A., and Hill, C. T., *Phys. Rev.*, **D49**, 409–425 (1994).
6. Di Pierro, M., and Eichten, E., *Phys. Rev.*, **D64**, 114004–24 (2001).
7. Bartelt, J., and Shukla, S., *Ann. Rev. Nucl. Part. Sci.*, **45**, 133–161 (1995).
8. Aubert, B., et al., *Phys. Rev. Lett.*, **90**, 242001–7 (2003).
9. Aubert, B., et al., *Nucl. Instrum. Meth.*, **A479**, 1–116 (2002).
10. Gronberg, J., et al., *Phys. Rev. Lett.*, **75**, 3232–3236 (1995).
11. Hagiwara, K., et al., *Phys. Rev.*, **D66**, 010001-974 (2002).
12. Besson, D., et al., *Arxiv:hep-ex/0305100* (2003).
13. Abe, K., *Arxiv:hep-ex/0307041* (2003).
14. Abe, K., *Arxiv:hep-ex/0307052* (2003).
15. Cho, P. L., and Wise, M. B., *Phys. Rev.*, **D49**, 6228–6231 (1994).
16. Cahn, R. N., and Jackson, J. D., *Arxiv:hep-ph/0305012* (2003).
17. Barnes, T., Close, F. E., and Lipkin, H. J., *Arxiv:hep-ph/0305025** (2003).
18. van Beveren, E., and Rupp, G., *Phys. Rev. Lett.*, **91**, 012003-6 (2003).
19. Bardeen, W. A., Eichten, E. J., and Hill, C. T., *Arxiv:hep-ph/0305049* (2003).
20. Cheng, H.-Y., and Hou, W.-S., *Arxiv:hep-ph/0305038* (2003).
21. Szczepaniak, A. P., *Arxiv:hep-ph/0305060* (2003).
22. Godfrey, S., *Arxiv:hep-ph/0305122* (2003).
23. Colangelo, P., and De Fazio, F., *Arxiv:hep-ph/0305140* (2003).